



Evidence of the role of contacts on the observed electron-hole asymmetry in graphene

B. Huard, N. Stander, J. A. Sulpizio, and D. Goldhaber-Gordon
Department of Physics, Stanford University, Stanford, California 94305, USA
 (Received 10 June 2008; published 4 September 2008)

We perform electrical transport measurements in graphene with several sample geometries. In particular, we design “invasive” probes crossing the whole graphene sheet as well as “external” probes connected through graphene side arms. The four-probe conductance measured between external probes varies linearly with charge density and is symmetric between electron and hole types of carriers. In contrast measurements with invasive probes give a strong electron-hole asymmetry and a sublinear conductance as a function of density. By comparing various geometries and types of contact metal, we show that these two observations are due to transport properties of the metal/graphene interface. The asymmetry originates from the pinning of the charge density below the metal, which thereby forms a p - n or p - p junction, depending on the polarity of the carriers in the bulk graphene sheet. Our results also explain part of the sublinearity observed in conductance as a function of density in a large number of experiments on graphene, which has generally been attributed to short-range scattering only.

DOI: [10.1103/PhysRevB.78.121402](https://doi.org/10.1103/PhysRevB.78.121402)

PACS number(s): 73.23.-b, 73.63.-b, 73.40.-c

Graphene, a crystalline monolayer of carbon, has a remarkable band structure in which low-energy charge carriers behave similarly to relativistic fermions, making graphene a promising material for both fundamental physics and potential applications.¹ Most interesting predicted transport properties require that charge carriers propagate with minimal scattering. Recently experimentalists have succeeded in reducing disorder^{2,3} and have shown the important role of nearby impurities on the mobility of charge carriers.^{4,5} In contrast, the effect of metallic contacts on transport has received little attention in experiments. For instance, most experiments show a clear difference between the conductances at exactly opposite densities, a phenomenon previously attributed to different scattering cross-sections off charged impurities for opposite carrier polarities only.^{6,7} In this Rapid Communication, we show that transport properties of the interface between graphene and metal contacts can also lead to such an asymmetry. This effect is due to charge transfer from the metal to graphene leading to a p - p or p - n junction in graphene, depending on the polarity of carriers in the bulk of the sheet. We also show that this effect leads to sublinear conductance as a function of gate voltage, which is traditionally attributed to short-range scattering.^{8–11} With a proper measurement geometry, we find conductivity linear in density up to at least $n=7 \times 10^{12} \text{ cm}^{-2}$ showing that short-range scattering plays a negligible role.

In order to investigate the properties of the graphene/metal interface, we used two types of metallic voltage probes (see inset in Fig. 1). “Invasive” probes (like a–e in Fig. 1) extending across the full graphene strip width are sensitive to contact and sheet properties, while “external” probes (like A–D in Fig. 1) connected to narrow graphene arms on the side of the strip are sensitive to sheet properties only. All the graphene samples described in this Rapid Communication are prepared by successive mechanical exfoliation of Highly Oriented Pyrolytic Graphite grade ZYA from General Electric (distributed by SPI) using an adhesive tape (3M Scotch Multitask tape with gloss finish). The substrate is a highly n -doped Si wafer, used as a gate (capacitance 13.6 nF cm^{-2}

from Hall-effect measurements), on which a layer of SiO_2 297 nm thick is grown by dry oxidation. Metallic probes are patterned using standard electron-beam lithography followed by electron-beam evaporation of metal (see Table I). Finally, the graphene sheets are etched in dry oxygen plasma (1:9 O_2 :Ar) into the desired shape. The voltage measurements between probes are performed in liquid helium at 4 K using a lock-in amplifier at a frequency between 10 and 150 Hz with a bias current of 100 nA. All samples were also measured in perpendicular magnetic fields up to 8 T and showed the quantum Hall plateaus characteristic of monolayer graphene. Most samples were additionally characterized by Raman scattering, in each case, showing the typical graphene spectrum (see supplementary material¹²).

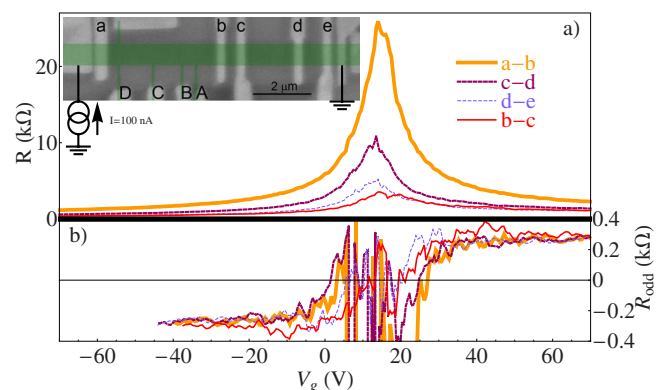


FIG. 1. (Color online) (a) Four-probe resistance calculated from voltages measured between invasive probes as a function of gate voltage, while a steady oscillating current of 100 nA runs along the whole graphene sheet. Inset: Scanning Electron Microscope image of the graphene sample TiAu1 connected to Hall probes (A–D) and invasive probes (a–e). For clarity, graphene has been colored according to topography measured by atomic force microscopy. (b) Given the charge neutrality gate voltage V_g^0 identified from quantum Hall-effect measurements (see text), we plot here the asymmetry between electrons and holes by showing the odd part of the resistance defined in Eq. (1).

TABLE I. Geometrical properties of the samples corresponding to Fig. 4. The measurements shown in Figs. 1–3 were performed on TiAu1. The type of metal used as a probe and its thickness is given here together with the length w of the graphene/metal interface.

Sample	Metal thickness	w (μm)
Pd1	Pd(30 nm)	0.4
Pd2	Pd(30 nm)	0.9
TiAu1	Ti(5 nm)/Au(25 nm)	0.8
TiAu2	Ti(3 nm)/Au(15 nm)	2.4

Figure 1 shows the four-probe resistances measured between four pairs of invasive probes in the sample TiAu1 as a function of gate voltage V_g . The resistance is maximal close to the value V_g^0 of the gate voltage where the average charge density is zero. In order to quantify the asymmetry between electron and hole transport, we plot in Fig. 1(b) the odd part of the resistance defined as

$$R_{\text{odd}}(\Delta V_g) = \frac{1}{2} [R(V_g^0 + \Delta V_g) - R(V_g^0 - \Delta V_g)]. \quad (1)$$

We determined the voltage V_g^0 with good precision using the sharp features of resistance as a function of density in the quantum Hall regime at 8 T. Two regimes of density can be distinguished. For low densities $n \lesssim 1.2 \times 10^{12} \text{ cm}^{-2}$, R_{odd} fluctuates widely. The extent of this fluctuating regime is consistent with the density of charged impurities $n_i = e(hc_2\mu)^{-1} \approx 0.5 \times 10^{12} \text{ cm}^{-2}$; one would calculate from the assumption that the mobility $\mu \approx 4600 \text{ cm}^2 \text{ V}^{-1} \text{ s}^{-1}$ (see Fig. 3) is dominated by scattering off-charged impurities where $c_2 \approx 0.1$ for graphene on SiO_2 .^{4,5} For larger densities $n \gtrsim 1.2 \times 10^{12} \text{ cm}^{-2}$, R_{odd} saturates to a finite value, corresponding to a higher resistance for electrons ($V_g > V_g^0$) than for holes ($V_g < V_g^0$). Such an asymmetry was previously predicted and observed in the presence of charge impurity scattering in graphene.^{4–7} In that case, the asymmetry comes from a difference between the scattering cross sections of positive and negative charge carriers on a charged impurity. Let us define two different resistivity functions $\rho_e(|n|)$ for electrons and $\rho_h(|n|)$ for holes as functions of density n . If this is the source of the asymmetry in resistance, the odd part R_{odd} should be given by $2R_{\text{odd}}(n) = [\rho_e(|n|) - \rho_h(|n|)]L/w$ for electrons ($n > 0$), where L is the distance between voltage probes and w is the width of the graphene strip. However, as can be seen in Fig. 2(b), the asymmetry of resistivity inferred in this way from our four measurements from Fig. 1 varies widely with changing L . On the contrary, if we associate R_{odd} with a specific interface resistance $r(n)$, all curves for different geometries collapse together [Fig. 2(a)]. Therefore, we propose a more general expression for R_{odd} ,

$$2R_{\text{odd}}(n) = \underbrace{[\rho_e(|n|) - \rho_h(|n|)]}_{\text{sheet property}} \underbrace{\frac{L}{w}}_{\ll} \underbrace{\frac{1}{w}}_{\text{interface}} + r(n) \frac{1}{w}. \quad (2)$$

Repeating the resistance measurements using external probes instead of invasive probes, we can get rid of the interface

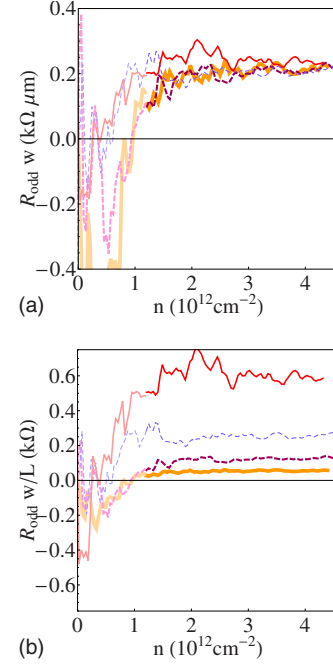


FIG. 2. (Color online) (a) Odd part of resistance normalized by the extent w of the metal/graphene interface for four pairs of invasive probes shown in the inset of Fig. 1 (same colors/grayscale). The fluctuating region at densities smaller than $1.2 \times 10^{12} \text{ cm}^{-2}$ has been grayed. The charge density n is measured using the classical Hall voltage between external probes, implying a capacitance of 13.6 nF cm^{-2} , consistent with the measured oxide thickness. (b) Same odd part of the resistance scaled by the ratio of the length w to the distance L between contacts.

term $r(n)/w$ in Eq. (2) and measure the sheet asymmetry only. To the precision of our measurements, $\rho_e/\rho_h = 1 \pm 0.03$ when averaged on all densities (Fig. 3 inset). The absence of asymmetry between ρ_e and ρ_h is in contrast with the ratio of about 1.20, which Chen *et al.*⁷ observed when graphene was exposed to chemical dopants. To understand this apparent discrepancy, let us consider the three proposed sources of scattering in graphene: short-range scatterers, charged impurities, and corrugation in the graphene sheet. First, short-range scatterers add a term ρ_s , almost independent of n to the resistivity. From Fig. 3, we can set an upper bound $\rho_s < 15 \text{ } \Omega/\square$, which is surprisingly small compared to other reported values.¹³ Charged impurities naturally lead to the observed linear dependence of conductivity on n , whereas corrugation requires a particular height correlation function to give the same behavior,^{8–11} which contradicts recent experiments.¹⁴ As has been predicted and shown experimentally, scattering off charged impurities of a given polarity occurs at a different rate for electrons and holes^{6,7} and it also shifts the voltage V_g^0 and decreases the mobility. However, both in our measurements and in those of Ref. 7 prior to doping, there is no asymmetry in the resistivity. This could be due to some equilibration between impurities of opposite polarities, but in this case, the difference in V_g^0 between the experiments is somewhat surprising and would be worthy of further investigation.

As we have seen, for invasive probes, R_{odd} scales in-

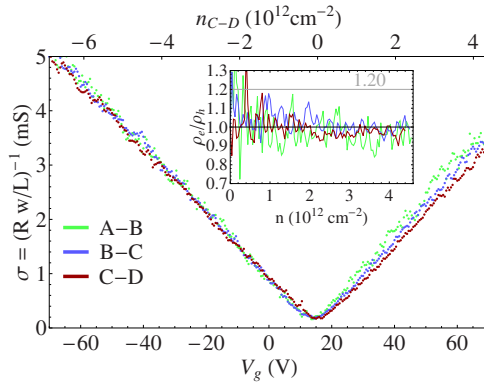


FIG. 3. (Color online) Conductivity as a function of gate voltage. Each color corresponds to a pair of probes identified by two letters in Fig. 1. The slope of these curves corresponds to a mobility of $\mu \approx 4600 \text{ cm}^2 \text{ V}^{-1} \text{ s}^{-1}$. Inset: given the charge neutrality gate voltage V_g^0 identified from quantum Hall-effect measurements (see text), we plot here the ratio between resistivities for electrons and holes as a function of carrier density. In contrast to the case of invasive probes, the average asymmetry is invisible to the precision of our measurement (note: the observed fluctuations are reproducible). The gray line corresponds to the ratio 1.20 as observed in Ref. 7 in the presence of chemical dopants.

versely with the extent w of the metal/graphene interface. Metallic probes in contact with graphene are expected to pin the charge density n_c in the graphene below the metal, thereby creating a density step along the graphene strip.^{15–17} The height of this step and the sign of n_c depend on the mismatch between the work functions of the metal and the graphene sheet. As we will see, for our choices of contact metal, the charge density in graphene is pinned to a negative value n_c (p type) below the metal. Thus depending on the polarity of the carriers in bulk graphene sheet, a p - n junction or a p - p junction develops close to the metal/graphene interface. We have shown elsewhere^{18,19} that the resistances associated with these junctions, for opposite values of the charge density n in the sheet, differ by an amount $r_{n_c}(n)/w$ where r_{n_c} depends only on n_c and on the length over which the density varies across the junction.^{20–23} This is consistent with the observed positive R_{odd} ; with n -type graphene below the contact one should observe a negative R_{odd} . If this is the origin of the observed asymmetry, R_{odd} should counter-intuitively decrease when the mismatch between metal and graphene work functions increases.

Figure 4 shows the function r_{n_c} measured in several graphene sheets contacted with two types of metal (see Table I). For Pd, which is expected to have a high work function ($\Phi_{\text{Pd}} \approx 5.1 \text{ eV} > \Phi_{\text{graphene}} = 4.5 \text{ eV}$) compared to the prediction for graphene,¹⁶ the function r_{n_c} decreases toward a small value. In contrast, for Ti covered with a layer of Au where the work-function mismatch should be smaller ($\Phi_{\text{Ti}} \approx 4.3 \text{ eV}$ and $\Phi_{\text{Au}} \approx 5.1 \text{ eV}$), the function r_{n_c} was larger at high densities n , suggesting that the densities n_c and n are of the same order of magnitude. We notice that for Pd, r_{n_c} decreases with n , whereas for Ti/Au it increases; but, it is hard to explain this increase since it would require knowing the potential profile close to the lead. Finally, as expected¹⁶

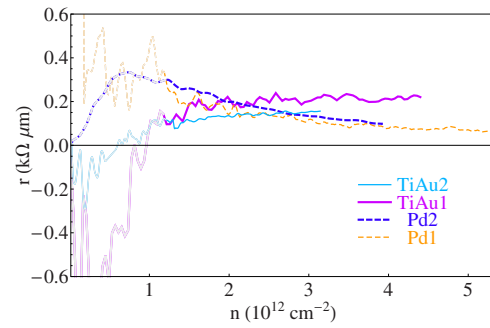


FIG. 4. (Color online) Odd part R_{odd} of the resistance scaled by the inverse width w^{-1} for various samples and metals described in Table I.

($\Phi_{\text{Al}} \approx 4.2 \text{ eV} < \Phi_{\text{graphene}}$), Ti/Al probes lead to the opposite doping: R_{odd} that we estimate from other works^{24,25} is negative.

Charge transfer from the metallic probes has yet another observable effect on transport. In Fig. 5(a), we show the conductance measured using invasive probes, scaled by the geometrical aspect ratio of each section. Even on the hole side ($V_g < V_g^0$) where there is no p - n junction, a sublinearity is striking when compared to the external probe measurement shown in the same figure. We find that there is a constant specific contact resistance λ such that $(R - \lambda/w)^{-1}$ is linear in density in the hole region [see Fig. 5(b)]. This contact resistance independent of density n can be attributed to a higher concentration of short-range scatterers near the contact (perhaps due to e -beam exposure during lithography) and/or to the region of constant density n_c near the contacts. In order to determine which effect is dominant, we compare the value of λ for the two different metals of Table I. We find that this resistance is small for Pd probes compared to Ti/Au

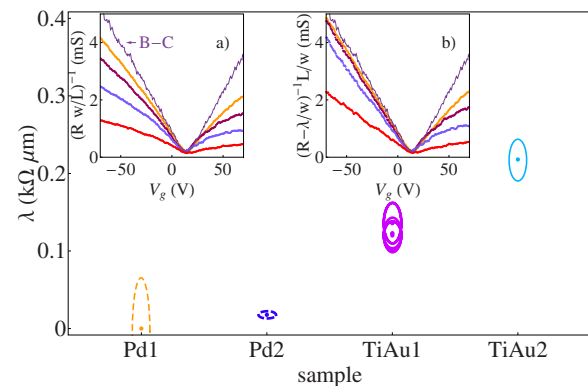


FIG. 5. (Color online) (a) From the resistance curves plotted in Fig. 1, we show the conductance scaled by the ratio w/L . The noninvasive measurement between probes B and C from Fig. 3 is plotted as a thin line for reference. (b) Subtracting $\lambda = 0.135 \text{ k}\Omega \mu\text{m}$ divided by the length w of the metal/graphene interface, each curve from (a) is linearized for the p -type carriers ($V_g < V_g^0$). Main panel: for each four-probe measurement on the samples from Table I, we plot here the specific resistance λ , which best linearizes the conductance as a function of gate voltage (see text). The best fit is obtained at the dot and the vertical size of the corresponding ellipse represents the uncertainty on λ .

probes, which is consistent with sublinearity coming from a region of larger constant density n_c for Pd than for Ti/Au, and not from short-range scatterers.

In conclusion, we have shown that all measurements using invasive metallic probes should exhibit an asymmetry between hole and electron conductances due to charge transfer at the graphene/metal interface. Similarly, invasive probes lead to a sublinearity in the conductance as a function of density, even in a four-probe geometry. In every experiment using invasive probes, one should consider these effects in the calculation of the conductivity from the resistance measurement and sample geometry. External probes do not have this issue and, here, reveal a conductance linear in density.

We thank D. Novikov, M. Fogler, and J. Cayssol for enlightening discussions. This work was supported by the MARCO/FENA program and by the Office of Naval Research under Grant No. N00014-02-1-0986. N.S. was supported by a William R. and Sara Hart Kimball Stanford Graduate Grant, J.A.S. was supported by a National Science Foundation Graduate Grant. This work was performed in part at the Stanford Nanofabrication Facility of NNIN supported by the National Science Foundation under Grant No. ECS-9731293. Critical equipment (SEM and AFM) was obtained partly through support from the Air Force Office of Scientific Research under Grants No. FA9550-04-1-0384 and No. F49620-03-1-0256.

-
- ¹A. H. Castro Neto, F. Guinea, N. M. R. Peres, K. S. Novoselov, and A. K. Geim, *Rev. Mod. Phys.* (to be published).
- ²K. I. Bolotin, K. J. Sikes, Z. Jiang, G. Fudenberg, J. Hone, P. Kim, and H. L. Stormer, *Solid State Commun.* **146**, 351 (2008).
- ³X. Du, I. Skachko, A. Barker, and E. Y. Andrei, arXiv:0802.2933 (unpublished).
- ⁴D. S. Novikov, *Phys. Rev. B* **76**, 245435 (2007).
- ⁵S. Adam, E. H. Hwang, V. M. Galitski, and S. D. Sarma, *Proc. Natl. Acad. Sci. U.S.A.* **104**, 18392 (2007).
- ⁶D. S. Novikov, *Appl. Phys. Lett.* **91**, 102102 (2007).
- ⁷J. H. Chen, C. Jang, M. S. Fuhrer, E. D. Williams, and M. Ishigami, *Nat. Phys.* **4**, 377 (2008).
- ⁸K. Nomura and A. H. MacDonald, *Phys. Rev. Lett.* **96**, 256602 (2006).
- ⁹T. Ando, *J. Phys. Soc. Jpn.* **75**, 074716 (2006).
- ¹⁰A. Fasolino, J. H. Los, and M. I. Katsnelson, *Nat. Mater.* **6**, 858 (2007).
- ¹¹M. Katsnelson and A. Geim, *Philos. Trans. R. Soc. London, Ser. A* **366**, 195 (2008).
- ¹²See EPAPS Document No. E-PRBMDO-78-R02836 for experimental and theoretical details. For more information on EPAPS, see <http://www.aip.org/pubservs/epaps.html>
- ¹³S. V. Morozov, K. S. Novoselov, M. I. Katsnelson, F. Schedin, D. Elias, J. A. Jaszczak, and A. K. Geim, *Phys. Rev. Lett.* **100**, 016602 (2008).
- ¹⁴M. Ishigami, J. H. Chen, W. G. Cullen, M. S. Fuhrer, and E. D. Williams, *Nano Lett.* **7**, 1643 (2007).
- ¹⁵R. Golizadeh-Mojarad and S. Datta, arXiv:0710.2727 (unpublished).
- ¹⁶G. Giovannetti, P. A. Khomyakov, G. Brocks, V. M. Karpan, J. van den Brink, and P. J. Kelly, *Phys. Rev. Lett.* **101**, 026803 (2008).
- ¹⁷S. Heinze, J. Tersoff, R. Martel, V. Derycke, J. Appenzeller, and P. Avouris, *Phys. Rev. Lett.* **89**, 106801 (2002).
- ¹⁸B. Huard, J. A. Sulpizio, N. Stander, K. Todd, B. Yang, and D. Goldhaber-Gordon, *Phys. Rev. Lett.* **98**, 236803 (2007).
- ¹⁹N. Stander, B. Huard, and D. Goldhaber-Gordon, arXiv:0806.2319 (unpublished).
- ²⁰V. V. Cheianov and V. I. Falko, *Phys. Rev. B* **74**, 041403(R) (2006).
- ²¹M. M. Fogler, D. S. Novikov, L. I. Glazman, and B. I. Shklovskii, *Phys. Rev. B* **77**, 075420 (2008).
- ²²M. I. Katsnelson, K. S. Novoselov, and A. K. Geim, *Nat. Phys.* **2**, 620 (2006).
- ²³L. M. Zhang and M. M. Fogler, *Phys. Rev. Lett.* **100**, 116804 (2008).
- ²⁴H. B. Heersche, P. Jarillo-Herrero, J. B. Oostinga, L. M. K. Vandersypen, and A. F. Morpurgo, *Nature (London)* **446**, 56 (2007).
- ²⁵P. Joyez (private communication).